ChemComm

Accepted Manuscript

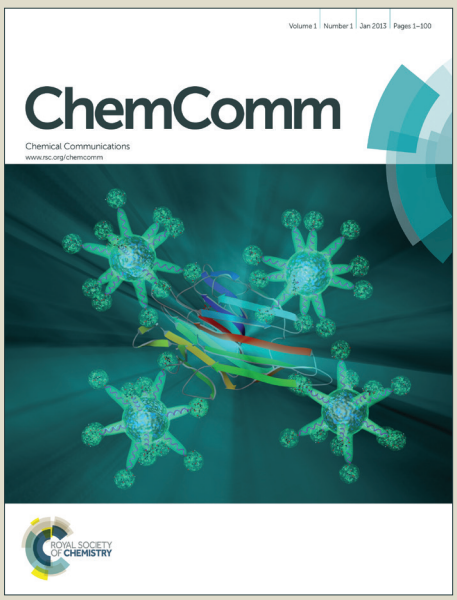

ROYAL SOCIETY OF CHEMISTRY

www.rsc.org/chemcomm

Journal Name

RSCPublishing

COMMUNICATION

Desorption of hydrogen from light metal hydrides: concerted electronic rearrangement and role of H···H interactions

Cite this: DOI: 10.1039/x0xx00000x

Received 00th January 2012,
Accepted 00th January 2012

DOI: 10.1039/x0xx00000x

www.rsc.org/

David J. Wolstenholme,* Matthew M. D. Roy, Michael E. Thomas and G. Sean McGrady*

A theoretical study of the desorption of hydrogen from rhombic Group 1 metal hydride dimers reveals a concerted reorganisation of the electron density for the M-H and H-H moieties as the reaction coordinate is traversed and a closed-shell H···H interaction evolves into a covalent H_2 bond. The central role played by homopolar dihydrogen bonding in this process is revealed and analysed.

The design of solid-state hydrogen storage materials often relies on building upon previous structural motifs, rather than understanding and exploiting the fundamental driving forces behind the evolution of hydrogen from these systems.[1,2] Thermal desorption of hydrogen from binary and complex metal hydrides necessitates simultaneous breaking of the M-H bonds and the formation of molecular H_2.[1] This concerted process depends strongly on subtle changes in the chemical bonding of these moieties as they traverse this reaction coordinate, and is reflected in the wide range of hydrogen desorption temperatures (T_{des}) exhibited by metal hydrides, for which an increase in the electronegativity of the metal leads to a contraction of its valence orbitals and a decrease in the ionicity of the M-H bonds.[3]

The apparent dependence of T_{des} on the electronegativity of the metal in binary hydrides prompted Edwards and Grochala to explore the relationship between this physical property and the standard reduction potential ($E°$) for the M^{n+}/M^0 couple.[3] These authors discovered an excellent correlation for a wide range of systems, which makes $E°$ an attractive metric for predicting T_{des} of many hydrides. Edwards and Grochala proposed that highly electropositive metals with significantly negative $E°$ values (< -2.3 V) desorb hydrogen at higher temperatures (> 330 °C), whereas moderately electropositive elements with higher potentials (-2.0 < $E°$ < -0.6 V) are characterised by lower T_{des} values (0-250 °C).[3] This trend is clearly observed for Group 2 hydrides, with T_{des} increasing as the metal becomes more electropositive (large negative $E°$ value; Table S1). In contrast, Group 1 hydrides are defined by the opposite trend, with the least electropositive metals displaying the highest T_{des} values, and with no clear trend in $E°$ values.[3] Such behaviour points to a more complex scenario for the Group 1 systems, with the key drivers behind the liberation of hydrogen remaining unclear.

The lack of a clear relationship between T_{des} and $E°$ values for Group 1 hydrides may be the result of different degrees of H···H interaction at key stages on the path to H_2 evolution, since previous gas-phase calculations have shown that related systems (*e.g.* SiH_4) engage in incipient homopolar dihydrogen bonding, even at early stages of this process.[4] This is not completely unexpected, as the vast majority of binary and complex metal hydrides release hydrogen via a reaction coordinate that necessarily involves the interaction of two hydridic moieties.[3] Notably, our recent studies of NH_3BH_3 and $LiNH_2BH_3$ revealed a similar hydride-hydride desorption pathway, in spite of the received wisdom that proton-hydride interactions are solely responsible for the evolution of hydrogen from amine-borane adducts and their derivatives.[5] This counter-intuitive behaviour is being shown to contribute to the liberation of hydrogen for a growing number of chemical hydrides, underscoring the importance of this type of interaction in the structures and reactivity of hydrogen-rich materials.[6]

The ability of two H^- ions to engage in an attractive interaction that leads to the eventual release of H_2 is remarkable, since decreasing the distance between these atoms is inherently repulsive in nature. Indeed, a previous computational study of the head-to-tail interaction of LiH dimers revealed extensive reorganisation of the electron density as the H···H distance is decreased, to a point where it is more energetically favourable to pair electrons covalently in the H···H internuclear region than to drive the two metal hydride components apart electrostatically.[7] This has prompted us to carry out a series of CCSD calculations on the related rhombic interactions of Group 1 hydride dimers (LiH **1**, NaH **2**, and KH **3**), as they proceed towards hydrogen desorption. This study has been augmented with a detailed topological analysis of the electron distribution for these dimers, using concepts espoused in the quantum theory of Atoms in Molecules (AIM).[8] This approach has afforded new and important insight into the pathways adopted by these systems, revealing strong correlations between the electronic structures of these dimers and the thermal properties that define the liberation of hydrogen from their solid-state counterparts.

The Group 1 hydrides each crystallise in the rock salt lattice F*m-3m* (#225), with the H^- ions occupying all octahedral holes in an fcc array.[9] This packing motif gives rise to local moieties that closely resemble the optimised structures of the rhombic dimers of **1**-**3**, which presents a logical starting point for mapping the release of hydrogen from these systems. The rhombic geometry of these dimers results in overall stabilisation (Fig. 1), in contrast to the previously

studied head-to-tail dimers, which are dominated by a significant repulsive component.[7] However, decreasing the H···H separation in **2** and **3** results in the eventual destabilisation of their cyclic configurations, as it becomes more favourable to adopt a linear orientation immediately prior to the liberation of H_2. In contrast, the rhombic dimer of **1** proceeds to H_2 release without such a structural rearrangement. These conclusions may have a bearing on the lack of a trend in the T_{des} values observed for these Group 1 hydrides.

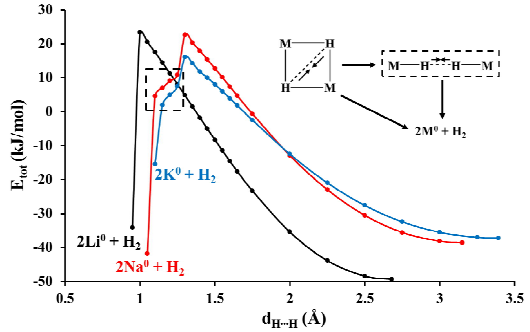

Fig. 1 Internal energy profiles for the rhombic MH dimers **1**-**3** *vs.* H···H distance.

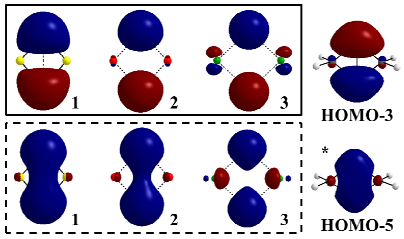

Fig. 2 Plots of the HOMO (above) and HOMO-1 (below) orbitals for the optimised structures of the rhombic dimers **1**-**3**, along with the HOMO-3 and HOMO-5 orbitals for Al_2H_6 for comparison. Isoelectronic density levels are 0.337 and 0.472* eÅ^{-3}.

In order to understand the differences in reactivity of these prototypical systems in more detail, we have analysed the changes in the electronic structures of the rhombic dimers **1**-**3**, as they progress through their hydrogen desorption reactions. The optimised structures form a delocalised bonding motif, with the two M-H moieties mutually connected through bridging H^- ions. Analysis of the molecular orbitals for these systems revealed a consistent pattern, with the HOMO in each case consisting of contributions from the 1s- and *n*p-orbitals of the H^- and M^+ ions, respectively (Fig. 2). These orbitals closely resemble the HOMO-3 of the Group 13 hydride dimer Al_2H_6 and are characteristic of 3-centre, 2-electron M-H-M bonding.[10] Moreover, the HOMO-1 orbitals for the rhombic dimers of **1**-**3** display favourable overlap of the two hydridic *n*s-orbitals, but the more compact 2s orbitals in **1** results in a more diffuse distribution of the density and a strengthening of the hydride-hydride interaction. In contrast, the corresponding orbitals for the dimers of **2** and **3** are defined by smaller and more localised densities, indicating a lack of homopolar dihydrogen bonding. These conclusions are confirmed through topological analysis of their electron distributions, with the molecular graph for the rhombic dimer of **1** revealing a bond path (BP) and a bond critical point (BCP) between the two H^- ions, whereas the dimers of the Na and K counterparts **2** and **3** display a ring critical point (RCP) in the H···H internuclear region. The presence of a BCP in **1** confirms that the density is a minimum along the H···H vector and is characteristic of two interacting atoms; in contrast the RCPs observed for **2** and **3** represent a minimum in the ring surface and a maximum perpendicular to this plane, excluding any H···H interactions.[8] These conclusions are consistent with a recent study of the solid-state counterparts of **1** and **2**, which found similar differences for LiH *vs.* NaH.[11]

The desorption of hydrogen from electropositive metal hydrides is generally assumed to proceed via an elongation and weakening of the M-H bonds, with a concomitant reduction in the H···H distance.[3] However, the energy profiles reported in Fig. 1 for the rhombic dimers of **1**-**3** point to a somewhat different pathway, with the accumulation of electron density at the BCP, $\rho_b(\mathbf{r})$, for the hydride-hydride interactions displaying a rapid increase as the H···H distance decreases (Fig. 3). This can be correlated with the changes in the HOMO-1 orbital for each of the dimers of **1**-**3**, with the density becoming more diffuse as the systems progress towards the formation of a covalent H-H bond. The superior overlap of the 2s-orbitals in the dimer of **1** allows the H-H bond formation to occur earlier, whereas this process is facilitated at a later stage of the reaction coordinate for **2** and **3**. These trends in the $\rho_b(\mathbf{r})$ values for the dimers of **1**-**3** indicate that homopolar H···H bonding acts as a tether, holding the two M-H components together in the early stages of these reactions, then playing a more influential role as these systems approach the formation and release of H_2.

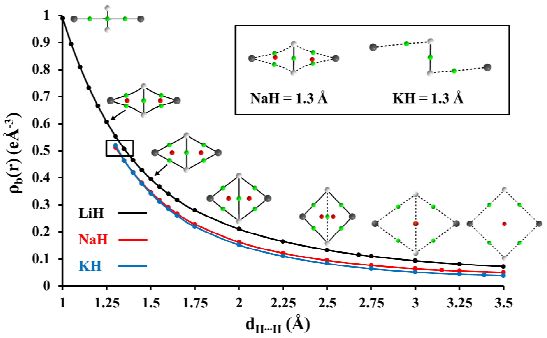

Fig. 3 Plot of $\rho_b(\mathbf{r})$ *vs.* H···H distance for the rhombic dimers **1**-**3**, along with salient molecular graphs. The bond (BCP) and ring (RCP) critical points are denoted as green and red spheres, respectively.

The ability of the H^- ions in these systems to establish a strong interaction in advance of M-H bond dissociation is clearly evident from an analysis of the $\rho_b(\mathbf{r})$ values. Nevertheless, this process is characterised by a complex interplay between competing interactions in the 3-centre, 2-electron bonding. The accumulation of electron density in the H···H internuclear region is accompanied by an initial strengthening of the M-H bonds. However, upon reaching the point at which the rhombic geometry is destabilised ($d_{H\cdots H}$ = 1.40 Å for **1**, 1.70 Å for **2**, and 1.75 Å for **3**), the M-H bonding weakens rapidly until bond dissociation occurs. This later stage occurs as the density of the hydride-hydride interactions becomes more diffuse in nature, giving rise to a more localised distribution in the vicinity of the M^+ ions (*i.e.* $2MH \rightarrow 2M^0 + H_2$). This feature is reflected in the changes to the molecular graphs observed for the dimers of **1**-**3**, with a strengthening of H···H bonding corresponding to a shift of the RCPs towards the cations, followed immediately by dissolution of the M-H bonds (Fig. 3). The larger size of the M^+ ions in the dimers of **2** and **3** forces this process to occur at an earlier stage in their reaction

coordinates, since decreasing the H···H separation to 1.3-1.4 Å corresponds to an acute H-M-H angle of ~35°. This geometry imposes a significant amount of strain on the electron distribution in these dimers, prompting two of the M-H bonds to break and switch to a head-to-tail orientation of the M-H moieties. This critical H-M-H angle is only reached at an H···H separation of 1.0 Å for **1**, at which point the H···H interactions have already accumulated more than 50% of the density corresponding to H_2 [$\rho_b(\mathbf{r})$ = 1.748 eÅ^{-3}].[12] These findings are fully consistent with the hitherto unexplained trend in T_{des} reported for LiH, NaH and KH, as the dimer of **1** maintains a rhombic geometry through to H_2 desorption, whereas those of **2** and **3** adopt a head-to-tail orientation prior to H_2 release.[3]

The presence of significant H···H bonding between the hydride moieties in the dimers of **1**-**3** is remarkable, on account of the significant electrostatic repulsion between the hydride moieties. The considerable redistribution of charge in these dimers occurs only after the hydride-hydride interactions have accumulated a substantial amount of electron density [$\rho_b(\mathbf{r})$ > 0.5 eÅ^{-3}], indicating that the repulsive electrostatic component is maintained - and even increased - as the reaction coordinates are traversed. This repulsive first-order contribution is overcome through significant polarisation of the H^- ions as they rapidly convert to a covalent H_2 moiety once the H···H distance falls within the appropriate range (Fig. 4).

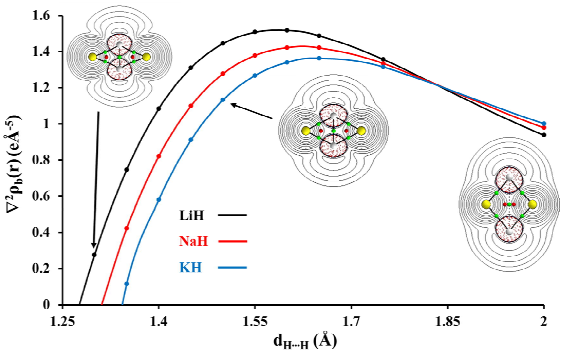

Fig. 4 $\nabla^2\rho_b(\mathbf{r})$ *vs.* H···H distance for the rhombic dimers **1**-**3**, with salient $\nabla^2\rho_b(\mathbf{r})$ maps for **1**. The positive (solid blue) and negative (dashed red) contours are plotted in increments of 2.4 x 10^{-2}, 4.8 x 10^n, 9.6 x 10^n, and 1.9 x 10^{n+1} (n = -2, -1, 0, 1, 2, and 3).

The $\rho_b(\mathbf{r})$ values for the homopolar dihydrogen interactions in the rhombic dimers of **1**-**3** reflect the accumulation of electron density in the H···H internuclear region prior to the formation of H_2, but this parameter fails to describe the transformation from closed-shell to covalent H···H interaction. More informative in this regard is the Laplacian of the electron density [$L(\mathbf{r}) = -\nabla^2\rho_b(\mathbf{r})$], which measures regions of charge depletion ($\nabla^2\rho_b(\mathbf{r}) > 0$) and concentration ($\nabla^2\rho_b(\mathbf{r}) < 0$), and hence provides both qualitative and quantitative metrics for the nature of the chemical bonding. The $\nabla^2\rho_b(\mathbf{r})$ values for the hydride-hydride interactions in the rhombic dimers of **1**-**3** display a gradual increase as the two H^- ions approach each other, followed by a rapid decrease in this parameter as the resulting four-centre moiety collapses and an H-H bond is formed (Fig. 4). This is consistent with closed-shell destabilisation of an intermolecular interaction, with the Na and K derivatives converting to a covalent H-H bond faster than their Li counterpart. Such behaviour is also reflected in the T_{des} values for these systems, with the heavier metal hydrides releasing hydrogen in the solid state at lower temperatures (~400 °C for **2** and **3** *vs* ~718 °C for **1**), and possessing lower activation barriers for the conversion to a covalent bond.[3]

In summary, gas-phase calculations of the rhombic dimers of Group 1 hydrides **1**-**3** and subsequent analysis of the electron densities thus obtained have afforded important insights into the process of H_2 evolution from these systems. Reorganisation of the electron density proceeds quite differently for the Na and K derivatives **2** and **3**, owing to the larger size of their M^+ ions, which leads to a more acute H-M-H angle at an earlier stage on the reaction coordinate and results in a sudden collapse of M-H bonding and reorganisation to a head-to-tail orientation of the M-H dimer prior to H_2 release. In contrast, the smaller Li^+ cations in the dimer of **1** allow for better overlap of the atomic orbitals responsible for the 3-centre, 2-electron bonding exhibited in the HOMO of this system, allowing this dimer to retain a rhombic geometry through to H_2 desorption. These findings are also in good agreement with the experimental T_{des} values reported for these hydrides, as the structural rearrangement in the Na and K dimers **2** and **3** facilitates the liberation of hydrogen faster than for their Li congener **1.** However, it would be dangerous to infer more about this correlation, since factors like crystal packing energies and the involvement of interactions such as M···H-Y bonding will also contribute to the overall behaviour of these systems.

Notes and references

Department of Chemistry, University of New Brunswick, P.O. Box 4400, Fredericton, N.B., Canada, E3B 5A3; e-mail: dwolsten@unb.ca and smcgrady@unb.ca

Electronic Supplementary Information (ESI) available: contains the topological and atomic properties of the electron density for **1**-**3** at various interval of their H···H bond formation, along with the corresponding values of the monomers. See DOI: 10.1039/c000000x/

1 S.-I. Orimo, Y. Nakamori, J.R. Eliseo, A. Züttel, C.M. Jensen, *Chem. Rev.*, 2007, **107**, 4111; L. George, S.K. Saxena, *Int. J. Hydrogen Energy*, 2010, **35**, 5454; I.P. Jain, P. Jain, A. Jain, *J. Alloy Compd*, 2010, **503**, 303; L. Klebanoff, "*Hydrogen Storage Technology Materials and Applications*"; CRC Press, Taylor & Francis Group: Boca Raton, Fl, U.S.A.; 2012.

2 C.W. Hamilton, R.T. Baker, A. Staubitz, I. Manners, *Chem. Soc. Rev.*, 2009, **38**, 279; A. Staubitz, A.P.M. Robertson, I. Manners, *Chem. Rev.*, 2010, **110**, 4079; Z. Huang, T. Autrey, *Energy Environ. Sci.*, 2012, **5**, 9257.

3 W. Grochala, P.P. Edwards, *Chem. Rev.*, 2004, **104**, 1283.

4 D.J. Aaserud, F.W. Lampe, *J. Phys. Chem. A*, 1997, **101**, 4114; S.P. Walch, C.E. Dateo, *J. Phys. Chem. A*, 2001, **105**, 2015.

5 D.J. Wolstenholme, J.T. Titah, F.N. Che, K.T. Traboulsee, J. Flogeras, G.S. McGrady, *J. Am. Chem. Soc.*, 2011, **133**, 16598; D.J. Wolstenholme, K.T. Traboulsee, Y. Hua, L.A. Calhoun, G.S. McGrady, *Chem. Commun.*, 2012, **48**, 2597.

6 D. Guerra, J. David, A. Restrepo, *Phys. Chem. Chem. Phys.*, 2012, **14**, 14892; X. Chen, F. Yuan, Y. Tan, Z. Tang, X. Yu, *J. Phys. Chem. C*, 2012, **116**, 21162.

7 A.M. Pendás, E. Francisco, M.A. Blanco, C. Gatti, *Chem. Eur. J.*, 2007, **13**, 9362.

8 R.F.W. Bader, "*Atoms in Molecules: A Quantum Theory*"; Oxford University Press: Oxford, U.K., 1990.

9 F. Yuh, , "*The metal-hydrogen system*"; Springer: New York, 1993.
10 X. Wang, L. Andrews, S. Tam, Mi.E. DeRose, M.E. Fajardo, *J. Am. Chem. Soc.*, 2003, **125**, 9218.
11 P. Sirsch, F.N. Che, J.T. Titah, G.S. McGrady, *Chem. Eur. J.*, 2012, **18**, 9476.
12 Optimisation of the H_2 molecule was carried out at the same level of approximation as the Group 1 hydride dimers **1**-**3**, CCSD/6-311++G(d,p).